Deoxysphingolipids activate cGAS-STING in colon cancer cells and enhance tumor immunity

Suchandrima Saha[1], Fabiola N. Valezquez[2], Fatemeh Dehpanah[1], Cungui Mao[2,3] and David C. Montrose[1,3]

[1]Department of Pathology, [2]Department of Medicine, Renaissance School of Medicine, Stony Brook University, Stony Brook, NY. [3]Stony Brook Cancer Center, Stony Brook, NY.

Corresponding Author: David C. Montrose, Department of Pathology, Renaissance School of Medicine, Stony Brook University, MART Building, 9M-0816, Lauterbur Dr., Stony Brook, NY 11794. Phone: 631-216-2927; Fax: 631-444-3424; Email: david.montrose@stonybrookmedicine.edu

Running title: Deoxysphingolipids and immunity

Keywords: colorectal cancer, mitochondria, chemokines

Grant Support: This work is supported in part by the Pilot Award Program for Team Science from Stony Brook Cancer Center (D.C.M. and C.M.).

Abstract

Bioactive sphingolipids (SLs) play critical roles in cellular function, including modifying the oncogenic potential of cancer cells. Depletion of the non-essential amino acid serine induces an intracellular shift from the generation of canonical SLs to non-canonical SLs known as deoxySLs, which can exert antitumor effects. Recent evidence has shown that restricting endogenous and exogenous sources of serine from cancer cells promotes antitumor immunity by activating the cyclic GMP-AMP Synthase-Stimulator of Interferon Genes (cGAS-STING) pathway. However, it is not known whether deoxySLs play a role in mediating this antitumor immune response. In this study, we demonstrated that depleting both externally supplied and internally synthesized serine from CT26 colon cancer cells maximally increased the levels of deoxySLs compared to removing either source alone. The ability of serine restriction to induce cytosolic accumulation of mitochondrial DNA (mtDNA) and subsequent activation of cGAS-STING components, including downstream Type I interferons (IFNs) was prevented by blocking deoxySL generation with the serine-palmitoyl transferase (SPT) inhibitor, myriocin. Direct administration of deoxysphinganine to cells induced mitochondrial dysfunction, in association with accumulation of cytosolic mtDNA, and increased expression of cGAS-STING components and Type I IFNs. A similar increase in IFNs was observed following mutation of SPT or supplementation of WT cells with alanine. Increasing deoxySLs in tumors through SPT mutation or feeding an alanine-enriched diet suppressed tumor growth in mice, while combining SPT mutation with a high alanine diet accentuated the antitumor effects. The observed tumor growth suppression was associated with increased infiltration of activated dendritic and cytotoxic T cells. Collectively, these findings reveal a novel role for deoxySLs in mediating antitumor immunity and provide support for the potential of using diet modification as an anticancer approach.

Introduction

Serine, a non-essential amino acid, plays key roles in a number of cellular functions, including metabolism, the antioxidant response and generation of bioactive sphingolipids (SLs) (1-4) As such, restricting it from cancer cells by depleting exogenous sources and/or inhibiting its synthesis, results in metabolic defects and subsequent antitumor effects, including increased sensitivity to anticancer therapy (5-15). In line with findings that altering cellular metabolism in cancer cells can modulate the immune microenvironment, recent evidence has shown that depleting serine in colorectal cancer (CRC) cells can enhance antitumor immunity (16). Specifically, combined restriction of both serine sources induced mitochondrial dysfunction, leading to cytosolic accumulation of mitochondrial DNA (mtDNA) and activation of the immunostimulatory cyclic GMP-AMP Synthase-Stimulator of Interferon Genes (cGAS-STING) pathway, enhancing antitumor immunity and efficacy of immunotherapy (16). Although these findings highlight a novel role for serine, the precise mechanism by which its depletion triggers these immune-stimulating events remains to be elucidated.

Sphingolipids (SLs) are a class of bioactive lipids generated by the enzymatic actions of serine-palmitoyl transferase (SPT) that serve both as structural components of cell membranes and organelles, as well as signaling molecules (17,18). In addition to their importance in maintaining normal cell function, SLs are also capable of mediating neoplasia (19,20). Although a strong amount of evidence exists for the role of canonical SLs in cancer pathogenesis, recent work highlights the importance of non-canonical SLs, known as deoxySLs, in cancer (21-23). DeoxySLs are produced when SPT utilizes alanine instead of serine as a substrate, which can result from mutation of SPT, depletion of serine availability or an increased ratio of alanine to serine (21-23). Notably, promoting deoxySL accumulation through multiple methods suppresses anchorage-independent cancer cell, cancer spheroid and tumor growth (21,23). However, these findings were made under immunodeficient conditions, leaving the unanswered question of whether inducing deoxySL accumulation impacts tumor immunity.

The current study tested the hypothesis that deoxySLs induce activation of cGAS-STING and enhance antitumor immunity following serine deprivation. Here, we found that blocking deoxySL production in CRC cells prevented mitochondrial dysfunction, release of mtDNA, activation of cGAS-STING components, and induction of Type I interferons (IFNs), under serine- deprived conditions. Deoxysphinganine (dSA) treatment induced mitochondrial defects and mitochondrial DNA (mtDNA) accumulation in the cytosol, and activated the cGAS-STING pathway, accompanied by increased Type I chemokine expression. A similar induction of Type I IFNs was observed when SPT was mutated or WT cells were exposed to excess alanine. Subsequent *in vivo* studies revealed that elevating intratumoral deoxySLs suppressed tumor growth, in association with increasing tumor-killing immune cell populations. Taken together, these findings support a novel mechanism by which deoxySLs exert anticancer effects.

Materials and Methods

Cell culture

Murine colorectal carcinoma CT26 cells were cultured in RPMI medium (Gibco) and human embryonic kidney 293T cells (ATCC) were cultured in DMEM (Gibco) and authenticated using the short tandem repeat profiling (ATCC). All cell lines were routinely tested for *Mycoplasma* using the MycoProbe Mycoplasma Detection Kit (R&D Biosystems) and all experiments were performed within 10 passages after thawing. The cells were maintained in medium containing 10% fetal bovine serum (FBS, Gibco) and 100 U mL^{-1} penicillin sodium and 100 μg mL^{-1} streptomycin sulfate (Gibco) at 37 °C under 5% CO_2. Complete (Comp) medium was prepared using MEM (Gibco) containing 10% dialyzed FBS (Gibco), 100 U mL^{-1} penicillin sodium and 100 μg mL^{-1} streptomycin sulfate, MEM vitamin mix, 4.5 g L^{-1} glucose, 0.4 mmol L^{-1} glycine and 0.4 mmol L^{-1} serine. Serine-deficient (Ser Def) medium was made with all components except for serine.

Cloning and lentiviral particle production

shRNAs targeting luciferase (*shLuc*) or murine *Psat1* (*shPsat1*) (clone #640) were cloned into a doxycycline (doxy)-inducible EZ-tet-pLKO-Puro vector (Addgene #85966). Lentiviral particles were generated by transfecting 293T cells with 1.5 µg ps-PAX2 (Addgene #12260), 0.5 µg pCMV-VSV-G (Addgene # 8454) plasmids along with 2 µg plasmid specifically targeting the genes of interest using Lipofectamine 2000. 48 and 72 h post transfection, viral supernatants were collected, and the target cells were transduced with viral supernatants containing polybrene (5 µg mL^{-1}). One day following infection, medium was changed, and selected with 5 µg mL^{-1} of puromycin for 48 h.

To generate inducible $SPTLC1^{WT}$ and $SPTLC1^{C133W}$ CT26 expressing cell lines, plasmids described in (21) were used. HEK293T cells were transfected with 250 ng of pCMV-VSVG, 750 ng of pCMV-dR8.2 and 1 µg of pCW57.1_SPTLC1_WT (Addgene Plasmid #181920) or pCW57.1_SPTLC1_C133W (Addgene Plasmid #181921) using Lipofectamine 2000. Viral supernatants were collected 48 h post transfection and CT26 cells were transduced with the viral supernatants containing polybrene (8 µg mL^{-1}). One day later, medium was changed, and cells were treated with 2 µg mL^{-1} puromycin for 72h to select for transduced cells. Engineered cells were cultured in respective media containing 10% tetracycline-free FBS (Genesee Scientific) and 100 U mL^{-1} penicillin sodium and 100 µg mL^{-1} streptomycin sulfate.

Analysis of mitochondrial membrane potential (MMP)

CT26 WT, *shLuc* or *shPsat1* cells were seeded at a density of 1×10^5 in 12-well plates. CT26 WT cells were treated with 500 nM of dSA for 6 h, while CT26 *shLuc* cells were treated with Comp media and *shPsat1* cells were given Ser Def media in the presence or absence of 500 nM myriocin for 24 h. Cells were harvested and incubated with 10 nM MitoTracker™ Deep Red (Invitrogen) for 20 min at 37°C. The cells were washed twice with PBS and counterstained with 1 µg mL^{-1} 4',6-diamidino-2-phenylindole (DAPI; Sigma-Aldrich) to distinguish between live

and dead cells. All the samples were acquired on an LSRII flow cytometer (BD) and analyzed using BD FACSDiva 9.0 software.

ROS measurements

CT26 WT cells were seeded at a density of 1×10^5 in 12-well plates and treated with 500 nM of dSA for 6 h. Cells were harvested, and incubated with CellROX green (Invitrogen) at a final concentration of 5 μM in serum-free DMEM for 30 min at 37°C. Cells were then washed twice with PBS, resuspended in cold PBS, counterstained with 1 μg mL^{-1} DAPI to distinguish live and dead cells. The samples were acquired on LSRII flow cytometer (BD) and analyzed using BD FACSDiva 9.0 software.

Immunofluorescence microscopy

Cells were grown on glass coverslips and following treatment and incubation, were washed twice with PBS and then fixed with 4% paraformaldehyde (Santa Cruz Biotechnology) for 15 mins. Cells were then permeabilized with 0.1% Tween20 and 0.01% Triton X-100 in PBS on ice, blocked in 2% BSA for 1 h, and incubated with primary antibodies specific for dsDNA (Santa Cruz, 1:200 dilution), LMNB (ab16048, Abcam, 1:500 dilution), COX4 (ab16056, Abcam, 1:300 dilution) or TFAM (GTX103231, GeneTex, 1:500 dilution). Next, cells were washed three times, 5 mins each and incubated with anti-mouse secondary antibody conjugated to Alexa Fluor 594 (ab150120, Invitrogen, 1:500 dilution), or anti-rabbit secondary antibody conjugated to Alexa Fluor 488 (A-11008, Thermo Fisher Scientific, 1:500 dilution) for 2 h at room temperature. Cells were washed three times with PBS, 5 mins each and counterstained using 1 μg mL^{-1} DAPI to identify the nucleus. Coverslips were then mounted onto slides using Fluoromount G Anti-fade (Southern Biotech) and images were captured using a Leica TCS SPF5 II confocal microscope at 100X magnification. Cytosolic dsDNA was quantified using NIH ImageJ (version 1.53k).

Immunoblotting

Cells were harvested and lysed using RIPA buffer (Sigma-Aldrich) supplemented

with 1 each of protease and phosphatase inhibitor tablet per 10 mL (ThermoFisher Scientific). The samples were incubated on ice for 15 mins, sonicated for 10 mins and centrifuged at 15,000g for 15 min at 4 °C. The supernatants were then collected and protein concentration was determined using the DC Protein Assay Reagent (Biorad). Equal amounts of proteins were resolved on 4- 20% Criterion TGX Precast Midi protein gradient gels (Biorad), transferred to nitrocellulose membranes, blocked with 5% BSA for 1 h at room temperature and incubated overnight at 4ºC with primary antibodies targeting phopsho-TBK1 (Cell Signaling, 5483, 1:1,000 dilution), TBK1 (Cell Signaling, 3504, 1:2,000 dilution), phopsho-STING1 (Cell Signaling, 19781, 1:2,000 dilution), STING1 (Cell Signaling, 13647, 1:2000 dilution) phopsho-IRF3 (Cell Signaling, 29047, 1:2,000 dilution), IRF3 (Cell Signaling, 4302, 1:2,000 dilution), PSAT1 (NBP1-32920, Novus Biologicals, 1:2,000 dilution), or anti-beta-Actin peroxidase (Sigma-Aldrich, A3854, 1:20,000 dilution). Following incubation with primary antibody, the membranes were incubated with horseradish peroxidase-conjugated anti-rabbit (Sigma, A0545, 1:3000 dilution) secondary antibody. Bands were visualized using Clarity Max Western ECL Substrate (Bio-Rad) on a C600 Gel Doc and Western Imaging System operated by cSeries capture v.1.6.8.1110 (Azure Biosystems).

Quantitative real-time PCR (qRT-PCR)

Total RNA from cells was isolated using QIAzol (Qiagen) and the quantity of RNA was determined using a NanoDrop ND-1000 spectrophotometer. 4000 ng of total RNA was used to prepare cDNA using oligo (dT) primers and reverse transcriptase (Quanta). Quantitative real-time PCR was performed using PowerTrack™ SYBR Green Master Mix (ThermoFisher) and gene-specific primers for mouse *Ifnb1* (fwd: 5'-AAGATCAACCTCACCTACAG-3'; rev: 5'-AAAGGCAGTGTAACTCTTCT-3'), Interferon-stimulated gene 15 (*Isg15*) (fwd: 5'-ACAGTGATGCTAGTGGTACA-3'; rev: 5'-AAGACCTCATAGATGTTGCT-3'), C-X-C motif chemokine ligand 10 (*Cxcl10*) (fwd: 5'-AAGTTTACCTGAGCTCTTTT-3'; rev: 5'-AGTATCTTGATAACCCCTTG-3'), and Chemokine (C-C motif) ligand 5 (*Ccl5*) (fwd: 5'-AGTGGGTTCAAGAATACATC-3'; rev: 5'- CTAGGACTAGAGCAAGCAAT-3'). Mouse Beta

actin (*ACTB*) was used as a housekeeping gene (fwd: 5'-GGCTGTATTCCCCTCCATCG-3'; rev: 5'-CCAGTTGGTAACAATGCCATGT-3'). Amplifications were run on the Applied Biosystems QuantStudio 7 Flex RT-PCR system and ΔΔCt method was used to calculate the relative expression.

In vivo studies

All experiments involving mice were conducted in accordance with the Institutional Animal Care and Use Committee of Stony Brook University. Six-week-old female BALB/c mice were purchased from Jackson Laboratory (Bar Harbor, ME). Mice were anaesthetized using isofluorane and 1×10^6 cells of SPTLC1^{WT} or SPTLC1^{C133W} CT26 cells were suspended in a 1:1 ratio of serum-free RPMI medium and matrigel were subcutaneously injected in the right flank. Mice were maintained in AIN-93G diet until they reached a palpable size of ~200 mm^3. Fourteen days post cell inoculation, the mice were randomized to either receive AIN-93G–based complete amino acid based diet or high alanine diet (Research Diets) (**Table S1**) for 8 days. All mice were administered 20 mg Kg^{-1} doxy by oral gavage every other day to induce shRNAs over the 8 day period. Tumor volume was measured manually using calipers.

Lipidomics

Cells were washed with cold PBS then scraped into 2 mL of cell extraction mix (2:3 of 70% Isopropanol: Ethanol). Samples were stored at -80°C until lipid extraction. Tumor samples stored at -80°C were transferred to Lysing Matrix A 2 mL tube containing garnet matrix and one ceramic sphere (MP Biomedicals) and minced with dissecting scissors in 500 µL of cell extraction mixture (2:3 of 70% Isopropanol: Ethanol). Samples were then homogenized using the FastPrep-24 lysis system (MP Biomedicals), centrifuged and supernatants were obtained. Next, cell extraction mixture was added, and samples were stored at -80°C until lipid extraction, as previously described (24).

For sphingolipid quantification, extracted samples from cells or tissues were spiked with 50 pmol of the corresponding internal standard and extracts were analyzed by the

Lipidomic Core Facility at Stony Brook University Medical Center, as described previously (25). Lipid levels were normalized to total inorganic phosphate.

Immune profiling

Tumors were excised, weighed, minced into 1-2 mm^3 pieces and then placed into a digestion solution containing 0.5 mg mL^{-1} collagenase D (Worthington Biochemical Corporation), 0.01 mg mL^{-1} DNase I (Sigma-Aldrich), and 0.5 mg mL^{-1}- dispase (Thermo Fisher Scientific) in RPMI medium for 30 min while shaking at 220 rpm at 37°C. Samples were vortexed and strained through a 70 μm cell strainer. The flow-throughs were collected and centrifuged at 1000 g for 5 min at 4°C. The pellets were resuspended in PBS and ACK lysis buffer (Invitrogen) was added to lyse the red blood cells. Samples were washed with FACS buffer (PBS + 2% FBS) followed by blocking of non-specific binding using FACS buffer for 30 min at room temperature. Live/dead staining was performed using LIVE/DEAD Fixable Aqua Dead Cell Stain (Invitrogen) at 1:500 dilution, and 1:200 dilution of fluorochrome-conjugated antibodies for specific cell surface markers were used as follows: CD45 (Biolegend, clone: 30-F11), CD3ε (Biolegend, clone: 145-2C11), CD8 (Biolegend, clone: 53-6.7), CD25 (Biolegend, clone: PC61), MHC class II (Biolegend, clone: M5/114.15.2), CD11c (Biolegend, clone: N418), and CD80 (Biolegend, clone: 16-10A1) for 30 mins at room temperature in dark. Next, the samples were washed in FACS buffer, fixed using 4% PFA in PBS for 20 mins, permeabilized with 0.5% Tween-20, blocked using 1% FBS diluted in permeabilization buffer for 15 mins and then stained with IFN-γ (Biolegend, clone: XMG1.2) and TNF-α (Biolegend, clone: MP6-XT22) at 1:200 dilution for 30 mins at room temperature in the dark. The samples were washed using FACS buffers then acquired on an LSRII flow cytometer (BD) and data were analyzed using the Kalluza C software (version1.1).

Statistical analysis

Differences in tumor growth were determined using an exponential regression model of tumor growth rate over time. The statistical comparisons in other assays were carried out using two-tailed Student's t-tests. Graphs were created using GraphPad Prism 10 and data

were plotted as mean +/- standard deviation. Statistical significance was set at $P < 0.05$, and all experiments were carried out with at least three biological replicates unless otherwise noted in the figure legend.

Results

DeoxySLs mediate mitochondrial dysfunction and activation of cGAS-STING following serine depletion

Our previous work demonstrated that depriving CRC cells of exogenous and endogenous serine activates the cGAS-STING pathway through cytosolic accumulation of mtDNA resulting from mitochondrial dysfunction (16). Given that serine loss also drives the accumulation of non-canonical deoxySLs, we posited that deoxySLs may be causally linked to these effects. Therefore, we first measured the levels of total deoxydihydroCeramides (deoxydhCeramides) in CT26 cells carrying doxy-inducible shRNAs targeting *Luciferase* (*shLuc*) or the serine synthesis enzyme *Psat1* (*shPsat1*) cultured in complete (Comp) or serine deficient (Ser Def) media, in order to deplete either or both sources of serine, or maintain serine sufficiency. Here, we found that while restricting endogenous or exogenous serine alone modestly increased deoxydhCeramide accumulation, depleting both sources maximally increased their levels (**Fig. 1A**). To mechanistically connect deoxySL generation with mitochondrially-mediated activation of cGAS-STING, cells were simultaneously deprived of serine and treated with the SPT inhibitor myriocin and a series of endpoints were examined. As shown in **Fig. 1B-E**, myriocin treatment reversed the decrease in MMP, increase in dsDNA accumulation, activation of cGAS-STING components and elevation in Type I IFN expression following serine depletion. Notably, treatment with deoxysphinganine (dSA), the immediate precursor to deoxydhCeramides, partially prevented the rescue of MMP elicited by myriocin, highlighting the deoxySL-specific effects of serine depletion (**Fig. 1B**). The ability of myriocin to prevent the increase in deoxydhCeramides under serine-deprived conditions was confirmed (**Fig. S1**). Taken together, these findings suggest that mitochondrial dysfunction and

subsequent cGAS-STING activation in serine-deprived cells are, at least in part, driven by accumulation of deoxySLs.

Exogenous administration or endogenous synthesis of deoxySLs activates the cGAS-STING pathway in CRC cells

To more directly examine whether deoxySLs are capable of inducing mitochondrial dysfunction and cytosolic accumulation of mtDNA, WT CT26 cells cultured in standard medium were treated with dSA, which resulted in decreased MMP and elevated reactive oxygen species (ROS), suggesting that mitochondrial dysfunction is occurring under these conditions (**Fig. 2A&B**). In parallel with these effects, increased cytosolic accumulation of dsDNA was observed (**Fig. 2C**). Moreover, approximately 90% of dsDNA colocalized with the mitochondrial markers COXIV and TFAM, while less than 10% associated with the nucleus, suggesting its mitochondrial origin (**Fig. 2D&E; Fig. S2**).

To evaluate whether the mitochondrial effects of dSA treatment were associated with activation of cGAS-STING, the expression of phosphorylated TBK1, STING1 and IRF3, were measured, which showed a strong increase at concentrations of 100 or 500 nM (**Fig. 3A**). In line with these findings, a dose-dependent increase in multiple immunostimulatory genes activated by phospho-IRF3 was observed, including *Ifnb1*, *Isg15*, *Cxcl10*, *Ccl5*, and *Mx1* (**Fig. 3B**). To establish whether other methods to increase deoxySLs induce a similar increase in Type I IFNs, we first generated CT26 carrying a doxy-inducible mutant form of SPT, SPTLC1_C133W, which preferentially uses alanine instead of serine as its substrate, thus generating deoxySLs (21,26,27). Here we found that inducing the SPT mutant significantly increased the expression of cGAS-STING responsive IFNs compared to inducing the WT form of SPT (**Fig 3C**). The ability to induce the mutant and WT forms of SPT by doxy treatment was confirmed along with demonstrating an ~60% increase in total deoxydhCeramides following induction of the mutant form (**Figs. S3 & S4**). Lastly, alanine supplementation in SPT WT cells was used as an additional method to promote deoxySL production, which showed a similar

increase in Type I IFNs (**Fig. 3D**). Collectively, these results support a causal role for deoxySLs in mediating cGAS-STING activation and production of Type I IFNs.

Inducing deoxySL production suppresses tumor growth and enhances intratumoral immune cell infiltration

Given the findings that deoxySL accumulation in CRC cells activates the immunostimulatory cGAS-STING pathway and accompanying increase in chemokines, we next examined whether these effects alter tumor biology. To test this concept, the SPT WT and C133W mutant CT26 cells described in Fig. 3 were inoculated into the flanks of syngeneic Balb/c mice, and after palpable tumors were established, mice were equally randomized to receive a control amino acid based diet or alanine enriched diet (**Table S1**) while inducing the WT or mutant forms of SPT. As shown in **Fig. 4A**, SPT mutant tumors exhibited suppressed growth compared to SPT WT tumors, an effect that was enhanced upon feeding an alanine enriched diet. High alanine diet feeding also suppressed WT tumor growth compared to WT tumors from mice fed a control diet, and to a level comparable to SPT mutant tumors (**Fig. 4A**). Total deoxydhCeramide levels were then measured in tumors at the end of the study. Here, we found that compared to WT tumors from mice fed control diet, the abundance of deoxydhCeramides doubled in mutant tumors from mice fed control diet and in WT tumors from mice fed high alanine diet, while combining SPT mutation with the high alanine diet increased levels by an additional 60% (**Fig. 4B**). We next determined whether tumor suppression and deoxySL accumulation were associated with alterations in immune cell populations within tumors. Flow cytometry-based measurements revealed that SPT mutant tumors from mice fed high alanine diet (which exhibited the strongest tumor suppression and highest deoxydhCeramide levels) exhibited an ~3-fold increase in the number of activated DCs and an approximate doubling in the number of activated CD8+ T cells, compared to SPT WT tumors from mice fed control diet (**Fig. 4C**). Collectively, these findings suggest that increasing tumor deoxySLs can induce antitumor immunity.

Discussion

Serine deprivation can promote antitumor immunity as well as induce the intracellular accumulation of deoxySLs, however, whether these effects are causally linked is not understood. Here, we show that deoxySLs play a role in activating the cGAS-STING pathway under serine-deprived conditions, which appears to be mediated by induction of mitochondrial dysfunction, leading to release of mtDNA. Further, multiple additional methods to induce deoxySL accumulation exert similar effects. Notably, both genetic and diet-mediated approaches to increase deoxySLs in tumors suppresses tumor growth in parallel with increasing infiltration of activated dendritic and T cells. Taken together, these findings suggest a novel role for non-canonical sphingolipids in driving antitumor immunity, providing potential alternative treatment options for CRC and other cancers.

Over the last several years, numerous studies have shown that depleting exogenous and/or endogenous serine exerts anticancer effects, including improving response to chemotherapy (5-15). Moreover, restricting both sources exerts more potent effects compared to limiting either source alone (8,9,11,12,28). Recent evidence extending upon these findings has shown that serine depletion triggers activation of the cGAS-STING pathway and accompanying induction of antitumor immunity (16). Notably, such effects only occurred when both exogenous and endogenous serine were depleted (16). The current work demonstrates a maximal increase in deoxySLs following restriction of both serine sources, compared to depleting only endogenous or exogenous serine, which may indicate a threshold of deoxySL accumulation that needs to be met in order to trigger mitochondrial dysfunction and subsequent activation of cGAS-STING. The fact that treatment with myriocin under serine-deprived conditions, which brought deoxydhCeramide levels close to what is found under control conditions, restored MMP, limited cytosolic accumulation of mtDNA, blocked cGAS-STING induction and expression of chemokines, suggests that deoxySLs play a key role in the observed cellular changes resulting from serine loss. The additional finding that direct treatment of cells with dSA, mutation of SPT or supplementation with alanine, all

independent methods to drive deoxySL accumulation, induced similar effects as serine deprivation further supports the role of deoxySLs in activating this pathway.

Although our findings suggest involvement of the immune system in the anticancer effects observed through multiple methods of inducing deoxySL accumulation, previous work has shown that spisulosine, a dSA stereoisomer isolated from the marine mollusc *Mactromeris polynyma*, can also exert direct toxic effects on a broad range of human cancer cell lines *in vitro* and *in vivo* (29). Further, more recent work demonstrated that accumulation of deoxySLs in cancer cells can inhibit anchorage independent growth of tumor cells *in vitro* and restrain tumor growth *in vivo*, all findings made under immunodeficient conditions (21,23). In light of this work, we cannot exclude the possibility that deoxySLs are mediating tumor suppression through direct toxic effects on the tumor cells themselves. Although it should be noted that compared to WT tumors from control diet-fed mice, protein expression of cleaved caspase 3 was not increased in SPT WT or mutant tumors from mice fed high alanine diets or SPT mutant tumors from control diet fed mice-all tumors that exhibited increased levels of deoxySLs (data not shown). Regardless, immune cell depletion experiments are needed to demonstrate that loss of immune cells abrogates the antitumor effects of deoxySLs, to fully support induction of antitumor immunity as a key mechanism by which tumor growth is suppressed in this context. In light of our findings suggesting that increasing deoxySLs activates the immunostimulatory pathway cGAS-STING as a result of mitochondrial dysfunction, a remaining question is the mechanism by which mitochondria become dysfunctional in this context. Studies in non-cancer cells have shown that exogenous administration of labeled dSA results in the accumulation of deoxydhceramide in both the mitochondria and ER (30). Therefore, it is possible that deoxySL accumulation in our system directly impacts mitochondrial function and/or induces ER stress, which in turn results in ER-mediated abnormalities in the mitochondria. Separate work showing that ER stress and accompanying disruptions in calcium homeostasis can increase calcium levels in the mitochondria, lend support to the latter hypothesis (31,32). Certainly more in-depth studies of both mitochondrial and ER biology in

the context of deoxySL accumulation in cancer cells are warranted to elucidate these important concepts.

It is well understood that a hereditary SPT mutation in humans results in neurotoxicity stemming from accumulation of deoxySLs in sensory neurons (33,34). Additional preclinical work demonstrates that long term feeding of a serine deficient or alanine-enriched diet results in neuropathy, resulting from accumulation of deoxySLs in sensory neurons (35,36). As such, although elevating deoxySLs in tumor cells exerts promising anticancer effects, likely through immune and non-immune mechanisms, concerns remain regarding the potential for associated toxicities. The work conducted in the current study reveals that short-term induction of deoxySLs exerts rapid tumor suppression and accompanying immune infiltration. And although formal analysis of neurological function was not performed, activity and gross motor function of mice in the experimental groups appeared to be equivalent to control mice. Given that longer-term deoxySL accumulation is responsible for the previously reported neuropathies, it is likely that the short-term induction used here will not induce deficits in neurologic function. Therefore, it may be possible that implementing this approach clinically on a short-term basis would be feasible, although the optimal approach for increasing tumor deoxSLs would need to be determined. Interestingly, direct administration of the dSA analogue enigmol through diet supplementation reduced intestinal tumor burden in *APC*$^{Min/+}$ mice and prostate cancer xenografts (37,38). Impressively, spisulosine was administered intravenously to patients with advanced cancer, and although these were phase I trials with the major goal of determining safety and pharmacokinetics, these studies highlight the ability to directly administer these lipids to patients (39,40). To the best of our knowledge, the current study is the first to demonstrate that feeding an alanine enriched diet increases deoxySLs in tumors and exerts tumor-suppressive effects. Given the potential ease of supplementing a patient's diet with amino acids, increasing intake of alanine may be a clinically feasible approach to drive deoxySL accumulation in tumors. Moreover, it is possible that such a dietary approach may better limit potential neurotoxicity given that tumor cells are nutrient avid and are therefore more likely to take up alanine compared to normal cells. Certainly, trials in cancer

patients to determine the safety and efficacy of increasing dietary alanine should be considered.

References

1. Locasale JW. Serine, glycine and one-carbon units: cancer metabolism in full circle. Nat Rev Cancer **2013**;13:572-83
2. Mattaini KR, Sullivan MR, Vander Heiden MG. The importance of serine metabolism in cancer. J Cell Biol **2016**;214:249-57
3. Yang M, Vousden KH. Serine and one-carbon metabolism in cancer. Nat Rev Cancer **2016**;16:650-62
4. Maceyka M, Spiegel S. Sphingolipid metabolites in inflammatory disease. Nature **2014**;510:58-67
5. Gao X, Lee K, Reid MA, Sanderson SM, Qiu C, Li S*, et al.* Serine Availability Influences Mitochondrial Dynamics and Function through Lipid Metabolism. Cell Rep **2018**;22:3507-20
6. Locasale JW, Grassian AR, Melman T, Lyssiotis CA, Mattaini KR, Bass AJ*, et al.* Phosphoglycerate dehydrogenase diverts glycolytic flux and contributes to oncogenesis. Nat Genet **2011**;43:869-74
7. Maddocks OD, Berkers CR, Mason SM, Zheng L, Blyth K, Gottlieb E*, et al.* Serine starvation induces stress and p53-dependent metabolic remodelling in cancer cells. Nature **2013**;493:542-6
8. Montrose DC, Saha S, Foronda M, McNally EM, Chen J, Zhou XK*, et al.* Exogenous and Endogenous Sources of Serine Contribute to Colon Cancer Metabolism, Growth, and Resistance to 5-Fluorouracil. Cancer Res **2021**;81:2275-88
9. Ngo B, Kim E, Osorio-Vasquez V, Doll S, Bustraan S, Liang RJ*, et al.* Limited Environmental Serine and Glycine Confer Brain Metastasis Sensitivity to PHGDH Inhibition. Cancer Discov **2020**;10:1352-73
10. Possemato R, Marks KM, Shaul YD, Pacold ME, Kim D, Birsoy K*, et al.* Functional genomics reveal that the serine synthesis pathway is essential in breast cancer. Nature **2011**;476:346-50
11. Sullivan MR, Mattaini KR, Dennstedt EA, Nguyen AA, Sivanand S, Reilly MF*, et al.* Increased Serine Synthesis Provides an Advantage for Tumors Arising in Tissues Where Serine Levels Are Limiting. Cell Metab **2019**;29:1410-21.e4
12. Tajan M, Hennequart M, Cheung EC, Zani F, Hock AK, Legrave N*, et al.* Serine synthesis pathway inhibition cooperates with dietary serine and glycine limitation for cancer therapy. Nat Commun **2021**;12:366
13. Falcone M, Uribe AH, Papalazarou V, Newman AC, Athineos D, Stevenson K*, et al.* Sensitisation of cancer cells to radiotherapy by serine and glycine starvation. Br J Cancer **2022**;127:1773-86
14. Labuschagne CF, van den Broek NJ, Mackay GM, Vousden KH, Maddocks OD. Serine, but not glycine, supports one-carbon metabolism and proliferation of cancer cells. Cell Rep **2014**;7:1248-58
15. Maddocks ODK, Athineos D, Cheung EC, Lee P, Zhang T, van den Broek NJF*, et al.* Modulating the therapeutic response of tumours to dietary serine and glycine starvation. Nature **2017**;544:372-6
16. Saha S, Ghosh M, Li J, Wen A, Galluzzi L, Martinez LA*, et al.* Serine Depletion Promotes Antitumor Immunity by Activating Mitochondrial DNA-Mediated cGAS-STING Signaling. Cancer Res **2024**;84:2645-59
17. Bartke N, Hannun YA. Bioactive sphingolipids: metabolism and function. J Lipid Res **2009**;50 Suppl:S91-6

18. Hannun YA, Obeid LM. Sphingolipids and their metabolism in physiology and disease. Nat Rev Mol Cell Biol **2018**;19:175-91
19. Janneh AH, Ogretmen B. Targeting Sphingolipid Metabolism as a Therapeutic Strategy in Cancer Treatment. Cancers (Basel) **2022**;14
20. Piazzesi A, Afsar SY, van Echten-Deckert G. Sphingolipid metabolism in the development and progression of cancer: one cancer's help is another's hindrance. Mol Oncol **2021**;15:3256-79
21. Cordes T, Kuna RS, McGregor GH, Khare SV, Gengatharan J, Muthusamy T*, et al.* 1-Deoxysphingolipid synthesis compromises anchorage-independent growth and plasma membrane endocytosis in cancer cells. J Lipid Res **2022**;63:100281
22. Truman JP, Ruiz CF, Montal E, Garcia-Barros M, Mileva I, Snider AJ*, et al.* 1-Deoxysphinganine initiates adaptive responses to serine and glycine starvation in cancer cells via proteolysis of sphingosine kinase. J Lipid Res **2022**;63:100154
23. Muthusamy T, Cordes T, Handzlik MK, You L, Lim EW, Gengatharan J*, et al.* Serine restriction alters sphingolipid diversity to constrain tumour growth. Nature **2020**;586:790-5
24. Bielawski J, Pierce JS, Snider J, Rembiesa B, Szulc ZM, Bielawska A. Sphingolipid analysis by high performance liquid chromatography-tandem mass spectrometry (HPLC-MS/MS). Adv Exp Med Biol **2010**;688:46-59
25. Bielawski J, Pierce JS, Snider J, Rembiesa B, Szulc ZM, Bielawska A. Comprehensive quantitative analysis of bioactive sphingolipids by high-performance liquid chromatography-tandem mass spectrometry. Methods Mol Biol **2009**;579:443-67
26. Gable K, Gupta SD, Han G, Niranjanakumari S, Harmon JM, Dunn TM. A disease-causing mutation in the active site of serine palmitoyltransferase causes catalytic promiscuity. J Biol Chem **2010**;285:22846-52
27. Bode H, Bourquin F, Suriyanarayanan S, Wei Y, Alecu I, Othman A*, et al.* HSAN1 mutations in serine palmitoyltransferase reveal a close structure-function-phenotype relationship. Hum Mol Genet **2016**;25:853-65
28. Buqué A, Galluzzi L, Montrose DC. Targeting Serine in Cancer: Is Two Better Than One? Trends Cancer **2021**;7:668-70
29. Faircloth G, Cuevas C. Kahalalide F and ES285: potent anticancer agents from marine molluscs. Prog Mol Subcell Biol **2006**;43:363-79
30. Alecu I, Tedeschi A, Behler N, Wunderling K, Lamberz C, Lauterbach MA*, et al.* Localization of 1-deoxysphingolipids to mitochondria induces mitochondrial dysfunction. J Lipid Res **2017**;58:42-59
31. Kumar V, Maity S. ER Stress-Sensor Proteins and ER-Mitochondrial Crosstalk-Signaling Beyond (ER) Stress Response. Biomolecules **2021**;11
32. Mohsin AA, Thompson J, Hu Y, Hollander J, Lesnefsky EJ, Chen Q. Endoplasmic reticulum stress-induced complex I defect: Central role of calcium overload. Arch Biochem Biophys **2020**;683:108299
33. Wilson ER, Kugathasan U, Abramov AY, Clark AJ, Bennett DLH, Reilly MM*, et al.* Hereditary sensory neuropathy type 1-associated deoxysphingolipids cause neurotoxicity, acute calcium handling abnormalities and mitochondrial dysfunction in vitro. Neurobiol Dis **2018**;117:1-14
34. Penno A, Reilly MM, Houlden H, Laurá M, Rentsch K, Niederkofler V*, et al.* Hereditary sensory neuropathy type 1 is caused by the accumulation of two neurotoxic sphingolipids. J Biol Chem **2010**;285:11178-87
35. Handzlik MK, Gengatharan JM, Frizzi KE, McGregor GH, Martino C, Rahman G*, et al.* Insulin-regulated serine and lipid metabolism drive peripheral neuropathy. Nature **2023**;614:118-24
36. Garofalo K, Penno A, Schmidt BP, Lee HJ, Frosch MP, von Eckardstein A*, et al.* Oral L-serine supplementation reduces production of neurotoxic deoxysphingolipids in mice and humans with hereditary sensory autonomic neuropathy type 1. J Clin Invest **2011**;121:4735-45

37. Symolon H, Bushnev A, Peng Q, Ramaraju H, Mays SG, Allegood JC*, et al.* Enigmol: a novel sphingolipid analogue with anticancer activity against cancer cell lines and in vivo models for intestinal and prostate cancer. Mol Cancer Ther **2011**;10:648-57
38. Garnier-Amblard EC, Mays SG, Arrendale RF, Baillie MT, Bushnev AS, Culver DG*, et al.* Novel synthesis and biological evaluation of enigmols as therapeutic agents for treating prostate cancer. ACS Med Chem Lett **2011**;2:438-43
39. Baird RD, Kitzen J, Clarke PA, Planting A, Reade S, Reid A*, et al.* Phase I safety, pharmacokinetic, and pharmacogenomic trial of ES-285, a novel marine cytotoxic agent, administered to adult patients with advanced solid tumors. Mol Cancer Ther **2009**;8:1430-7
40. Schöffski P, Dumez H, Ruijter R, Miguel-Lillo B, Soto-Matos A, Alfaro V*, et al.* Spisulosine (ES-285) given as a weekly three-hour intravenous infusion: results of a phase I dose-escalating study in patients with advanced solid malignancies. Cancer Chemother Pharmacol **2011**;68:1397-403

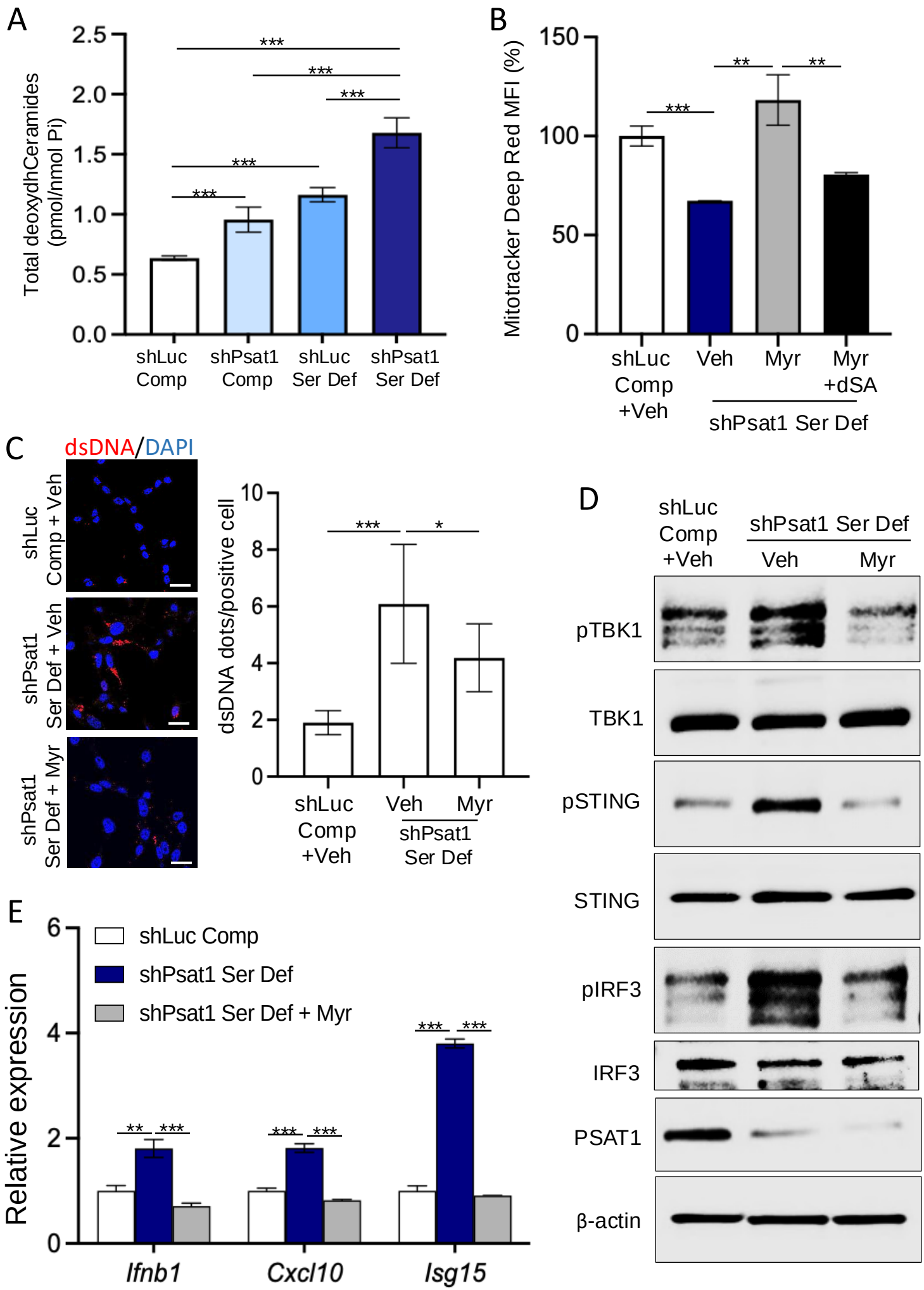
A
Total deoxydhCeramides (pmol/nmol Pi)
2.5
2.0
1.5
1.0
0.5
0.0
***
***
***
***
***
shLuc Comp
shPsat1 Comp
shLuc Ser Def
shPsat1 Ser Def
B
Mitotracker Deep Red MFI (%)
150
100
50
0
***
**
**
shLuc Comp +Veh
Veh
Myr
Myr +dSA
shPsat1 Ser Def
C
dsDNA/DAPI
shLuc Comp + Veh
shPsat1 Ser Def + Veh
shPsat1 Ser Def + Myr
dsDNA dots/positive cell
10
8
6
4
2
0
***
*
shLuc Comp +Veh
Veh
Myr
shPsat1 Ser Def
D
shLuc Comp +Veh
shPsat1 Ser Def
Veh
Myr
pTBK1
TBK1
pSTING
STING
pIRF3
IRF3
PSAT1
β-actin
E
Relative expression
6
4
2
0
shLuc Comp
shPsat1 Ser Def
shPsat1 Ser Def + Myr
**
***
***
***
***
***
Ifnb1
Cxcl10
Isg15

Figure 1. DeoxySL accumulation activates the cGAS-STING pathway following serine depletion. (A) CT26 cells carrying doxycycline (doxy)-inducible shRNAs targeting luciferase (*shLuc*) or Psat1 (*shPsat1)* were cultured in complete (Comp) or serine deficient (Ser Def) medium, as indicated, and treated with doxy for 24 h. The abundance of total deoxydihydroCeramides (deoxydhCeramides) were measured in cells by mass spectrometry. B) *shLuc* or *shPsat1* cells were cultured in Comp or Ser Def medium, respectively, and treated with 500 nM myriocin or vehicle or myriocin in combination with 500 nM deoxysphinganine (dSA), as indicated, and mitochondrial membrane potential was determined by flow cytometry after staining with Mitotracker Deep Red. C) *shLuc* and *shPsat1* cells were cultured in Comp or Ser Def medium, respectively, and treated with myriocin or vehicle, as indicated, and cytosolic dsDNA accumulation was assessed by immunofluorescence using a dsDNA-specific antibody (red color). Representative images (left side) and number of cytosolic dsDNA puncta per cell was quantified (right), are shown. D) *shLuc* and *shPsat1* cells were treated as described in panel C and western blotting was carried out to probe for the indicated proteins. E) *shLuc* and *shPsat1* cells were treated as described in panel C and qRT-PCR was carried out to determine expression of the indicated genes. Data are reported as relative to the shLuc Comp + Veh group. *P≤0.05; **P≤0.01; ***P≤0.001.

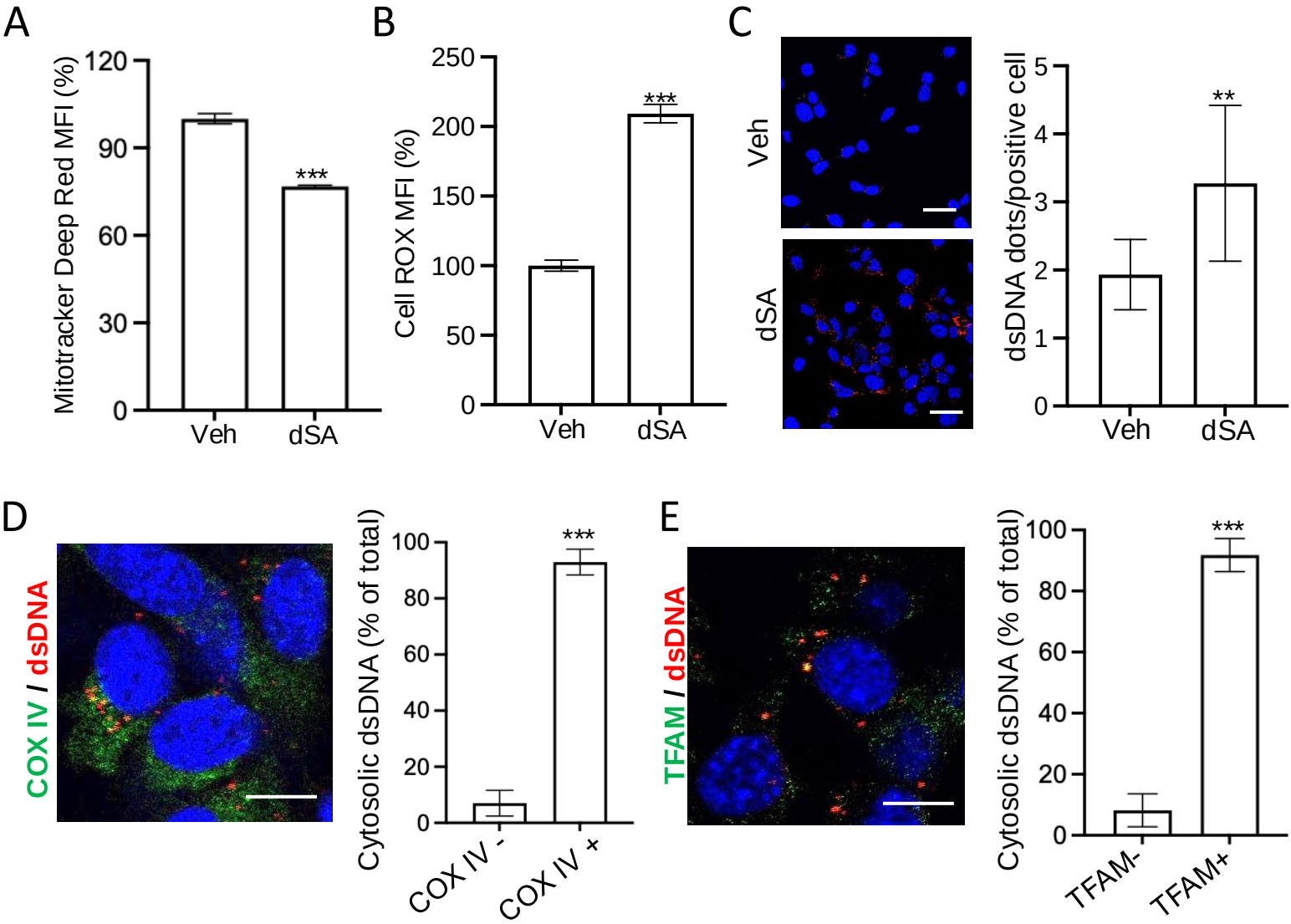

Figure 2. Deoxysphinganine (dSA) treatment induces mitochondrial dysfunction and release of mitochondrial DNA. A-B) WT CT26 cells were treated with 500 nM dSA or vehicle for 6 hrs and mitochondrial membrane potential was determined by flow cytometry after staining with Mitotracker Deep Red (A) and reactive oxygen species levels were determined by flow cytometry after staining with CellROX (B). Values in the vehicle group were set to 100% and values for other conditions are displayed as relative to that group. C-E) Cells were treated as described in Panels A and B and cytosolic dsDNA accumulation was assessed by immunofluorescence using a dsDNA-specific antibody (red color). Representative images (left side) and percent of cells that were positive for cytosolic dsDNA was quantified (right), are shown (C). Cells were co-stained for dsDNA and COXIV and representative images (left side) and quantification of the percent of cytosolic dsDNA dots in proximity to COXIV (right side), are shown (D). Cells were stained for dsDNA and TFAM and representative images (left side) and quantification of the percent of cytosolic dsDNA co-localizing with TFAM, are shown (E). DAPI (blue color) was used to stain the nuclei in all images. Scale bar = 10 μm. **P≤0.01; ***P≤0.001.

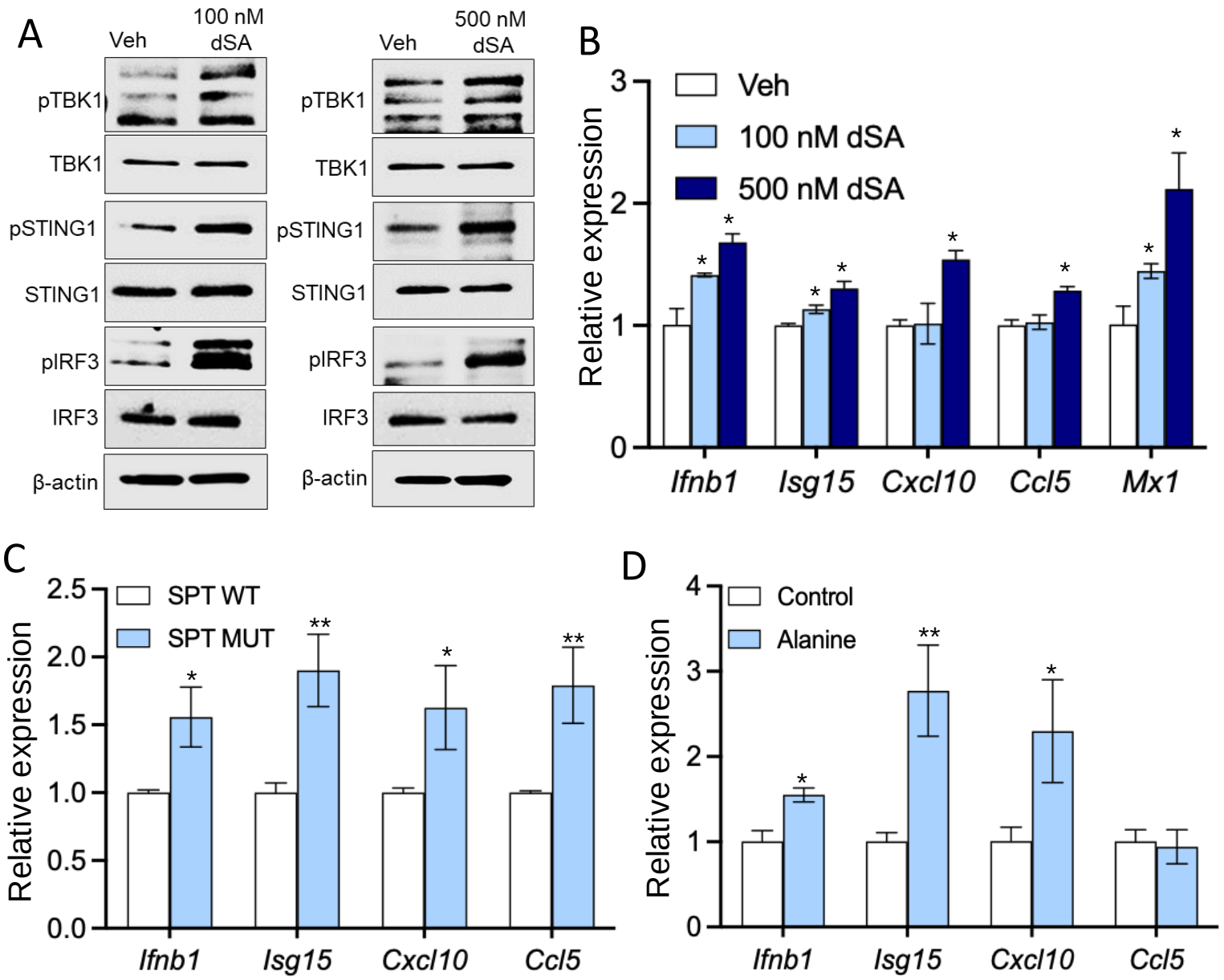

Figure 3. DeoxySLs induce the cGAS-STING pathway. A-B) WT CT26 cells were treated with 100 or 500 nM dSA or vehicle for 18 hrs and western blotting was carried out to probe for the indicated proteins (A) and qRT-PCR was carried out to determine expression of Type I IFNs (B). C) CT26 cells carrying doxycycline (doxy)-inducible WT or mutant SPT were treated with doxy for 24 hrs then qRT-PCR was carried out to determine expression of the indicated genes. D) CT26 cells carrying WT SPT were cultured under control or high alanine (3.2 mM) conditions for 48 hrs and qRT-PCR was carried out to determine expression of the indicated genes. *P≤0.05; **P≤0.01.

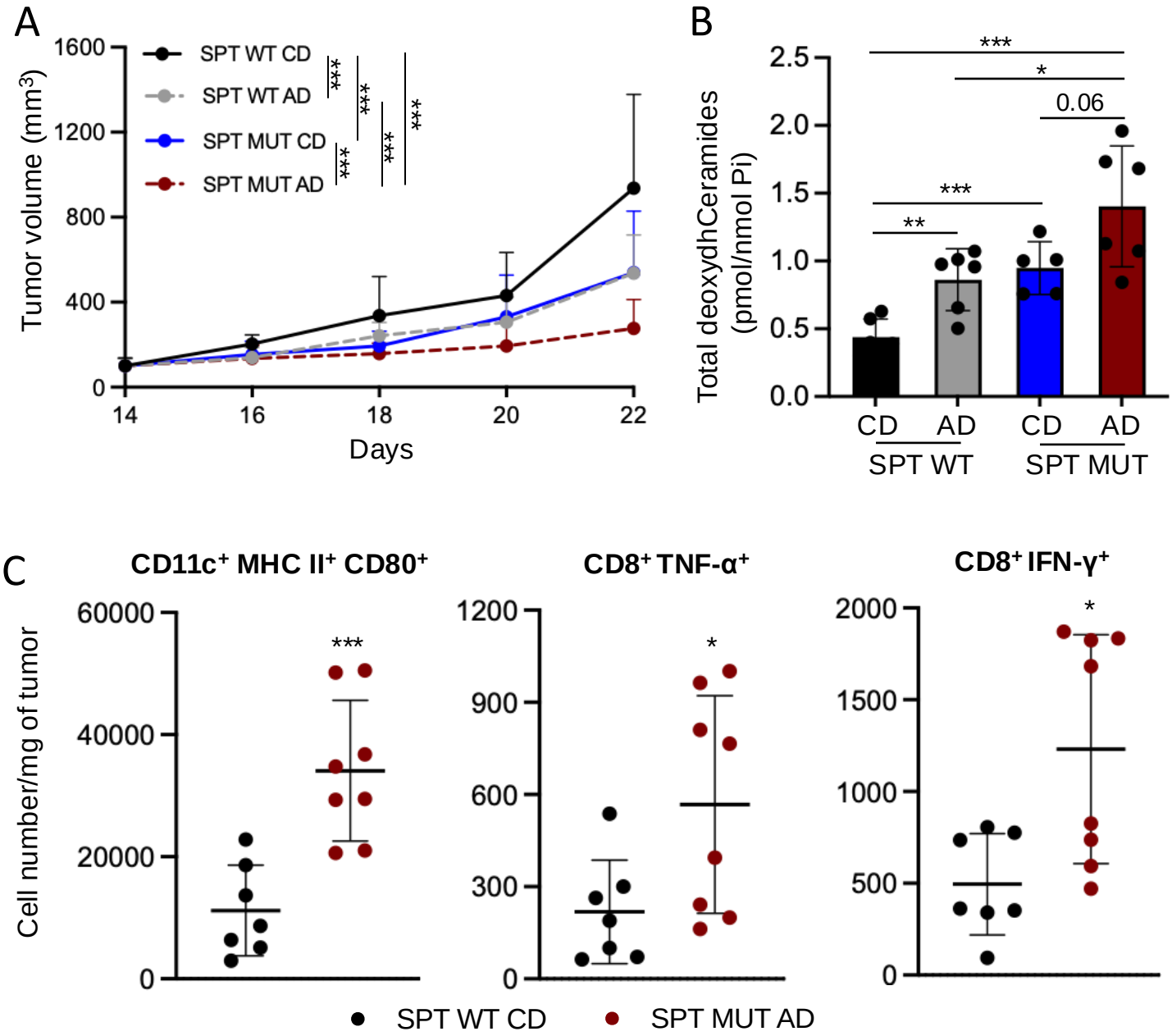

Figure 4. Increasing deoxySLs suppresses tumor growth and enhances immune cell influx. CT26 cells carrying doxycycline (doxy)-inducible WT or mutant SPT were inoculated into the flanks of Balb/c mice and tumors were allowed to grow to a palpable size over 2 weeks. Half of the mice bearing either tumor type were fed control amino acid based diet (CD) and the other half were fed high alanine diet (AD), while all mice received doxy by oral gavage every other day (n=7-8/group). A) Tumor size was measured every other day and calculated as percent change compared to day 14. B) Total deoxydihydroceramide (deoxydhceramide) levels were measured in tumors on day 22. C) Flow cytometry was carried out on single cell preparations of tumors from select groups on day 22 and the number of activated dendritic cells (CD11c$^+$ MHCII$^+$ CD80$^+$) and cytotoxic T cells (CD8$^+$ TNF-α$^+$; CD8$^+$ IFN-γ$^+$) were quantified, as indicated. *P≤0.05; **P≤0.01; ***P≤0.001.